BIOCHEMISTRY
including biophysical chemistry & molecular biology
Article

Biochemistry **2009,** *48,* 5339–5349 5339
DOI: 10.1021/bi900438w

Enzymatic Characterization of c-Met Receptor Tyrosine Kinase Oncogenic Mutants and Kinetic Studies with Aminopyridine and Triazolopyrazine Inhibitors

Sergei L. Timofeevski, Michele A. McTigue, Kevin Ryan, Jean Cui, Helen Y. Zou, Jeff X. Zhu, Fannie Chau, Gordon Alton, Shannon Karlicek, James G. Christensen, and Brion W. Murray*

Pfizer Global Research and Development, La Jolla, Pfizer Inc., 10777 Science Center Drive, San Diego, California 92121,

Received March 13, 2009; Revised Manuscript Received April 23, 2009

ABSTRACT: The c-Met receptor tyrosine kinase (RTK) is a key regulator in cancer, in part, through oncogenic mutations. Eight clinically relevant mutants were characterized by biochemical, biophysical, and cellular methods. The c-Met catalytic domain was highly active in the unphosphorylated state (k_{cat} = 1.0 s^{-1}) and achieved 160-fold enhanced catalytic efficiency (k_{cat}/K_m) upon activation to 425000 s^{-1} M^{-1}. c-Met mutants had 2−10-fold higher basal enzymatic activity (k_{cat}) but achieved maximal activities similar to those of wild-type c-Met, except for Y1235D, which underwent a reduction in maximal activity. Small enhancements of basal activity were shown to have profound effects on the acquisition of full enzymatic activity achieved through accelerating rates of autophosphorylation. Biophysical analysis of c-Met mutants revealed minimal melting temperature differences indicating that the mutations did not alter protein stability. A model of RTK activation is proposed to describe how a RTK response may be matched to a biological context through enzymatic properties. Two c-Met clinical candidates from aminopyridine and triazolopyrazine chemical series (PF-02341066 and PF-04217903) were studied. Biochemically, each series produced molecules that are highly selective against a large panel of kinases, with PF-04217903 (>1000-fold selective relative to 208 kinases) being more selective than PF-02341066. Although these prototype inhibitors have similar potencies against wild-type c-Met (K_i = 6−7 nM), significant differences in potency were observed for clinically relevant mutations evaluated in both biochemical and cellular contexts. In particular, PF-02341066 was 180-fold more active against the Y1230C mutant c-Met than PF-04217903. These highly optimized inhibitors indicate that for kinases susceptible to active site mutations, inhibitor design may need to balance overall kinase selectivity with the ability to inhibit multiple mutant forms of the kinase (penetrance).

The receptor tyrosine kinase (RTK)[1] c-Met was first identified as a proto-oncogene and is the only known high-affinity receptor for the hepatocyte growth factor (HGF, scatter factor) (*1*, *2*). The c-Met receptor is a heterodimer composed of an extracellular α-chain and a transmembrane β-chain that are proteolytic cleavage products originating from a single gene (*3*). The β-chain contains an extracellular domain, a transmembrane domain, and a cytoplasmic domain. The cytoplasmic domain is further segmented into a juxtamembrane domain, a catalytic domain, and a C-terminal docking domain. Interestingly, c-Met is thought to be unique to vertebrates because there are no orthologs in *Drosophila melanogaster* or *Caenorhabditis elegans* (*4*). Binding of HGF ligand to the c-Met extracellular domain results in receptor multimerization and phosphorylation of tyrosine residues in the intracellular c-Met domains. Similar to those of other RTKs, the kinase activity of c-Met has been shown to be regulated by autophosphorylation, with the phosphorylated c-Met receptor reported to have several-fold more kinase activity than the dephosphorylated receptor (*5*). Autophosphorylation of the catalytic subunit was shown to include phosphorylation of activation loop tyrosine residues 1234 and 1235 (*6*) with an additional catalytic domain site more recently proposed (tyrosine residue 1194) (*7*). The autophosphorylation reaction has been reported to proceed through sequential phosphorylation events (*8*). Kinetic studies of the recombinantly expressed cytoplasmic domain of c-Met have reported that the $K_{m,ATP}$ was 70.4 μM while the k_{cat} was only 0.0095 s^{-1} (*9*). As reported, c-Met is not a very potent catalyst (k_{cat}/K_m = 140 s^{-1} M^{-1}). More recent kinetic modeling studies of the c-Met regulation

*To whom correspondence should be addressed: Pfizer Global Research and Development, La Jolla, Pfizer Inc., 10777 Science Center Dr., San Diego, CA 92121. Telephone: (858) 622-6038. Fax: (858) 526-4240. E-mail: brion.murray@pfizer.com.

[1]Abbreviations: BCA, bicinchoninic acid; BOAP, 3-benzyloxy-2-aminopyridine; DMSO, dimethyl sulfoxide; DSF, differential scanning fluorimetry; DTT, dithiothreitol; EDC, *N*-ethyl-*N*′-[3-(dimethylamino)propyl]carbodiimide; EDTA, ethylenediaminetetraacetic acid; HBSS, Hank's Balanced Salt Solution; HEPES, 4-(2-hydroxyethyl)-1-piperazineethanesulfonic acid; HGF, hepatocyte growth factor; IEF, isoelectric focusing; IPTG, isopropyl β-D-1-thiogalactopyranoside; MES, 2-(*N*-morpholino)ethanesulfonic acid; MALDI-TOF, matrix-assisted laser desorption ionization time-of-flight; Met2, c-Met activation loop peptide; MOI, multiplicity of infection; MS, mass spectrometry; nano-ESI, nanoelectrospray ionization; NHS, *N*-hydroxysuccinimide; PFU, pock-forming units; RTK, receptor tyrosine kinase; TAP, triazolopyrazine; TCEP, tris(2-carboxyethyl)phosphine hydrochloride; TFA, trifluoroacetic acid; TMB, 3,3′,5,5′-tetramethylbenzidine; Tris-HCl, tris(hydroxymethyl)aminomethane hydrochloride; WT, wild type.

 Published on Web 04/24/2009

predict a 10-fold increase in the catalytic efficiencies upon autophosphorylation (*10*). The proposed model of c-Met regulation predicts that the rate of phosphorylated c-Met accumulation is directly proportional to the c-Met k_{cat} value. As such, basic elements of c-Met activation and activity have been reported.

The c-Met RTK has been implicated in the progression of a variety of human cancers and is an emerging target for therapeutic intervention (*3*, *11*). In cancer, inappropriate c-Met signaling has been shown to occur through multiple mechanisms: receptor overexpression, amplification, and mutation (*3*, *11*, *12*). Germline and somatic mutations to the c-Met proto-oncogene were initially identified in humans in 1997 (*13*), with other mutations subsequently identified (*14*−*17*). Interestingly, different mutations in the c-Met kinase domain affected the type of cancers that developed in vivo (*18*). One such mutation is the Y1230C germline mutation which predisposes humans to hereditary renal cell carcinoma (*14*). The initial biochemical characterization of oncogenic mutations showed that a subset of mutant c-Met kinase constructs had more activity (~3-fold increase) which correlated with tumorigenesis when cells were transplanted into immunocompromised mice (*15*). Five different oncogenic c-Met mutant constructs were transfected into cells and shown to have differential levels of tyrosine phosphorylation that did not correlate with the constant increase in kinase activity (~3-fold enhancements) (*15*). These results indicate that phosphorylation events may or may not be influencing kinase activity. Although the oncogenic mutations of c-Met have been well-documented, other mechanisms for pathway activation have been reported to occur at a higher frequency in tumors (*11*, *19*).

A number of hypotheses about the role of the oncogenic c-Met mutations in cancer have been proposed. Studies of a subset of activating mutations (L1213V and M1268T) indicate that they circumvent the normally stringent requirement for dual phosphorylation of the c-Met activation loop and stabilize an active conformation of the kinase (*16*). Others report that oncogenic mutants (D1226H/N, D1250T, and Y1235D) overcome the need for a second phosphorylation event on tyrosine residue 1234 (*7*, *8*). Biophysical analysis of the c-Met activating mutant Y1235D indicated it conferred constitutive activity, was not influenced by the autophosphorylation of Y1234, but achieved lower activity than the fully activated wild-type c-Met (*7*). A related hypothesis is that the oncogenic mutations (M1250T and D1228H) decrease the threshold for kinase activation (*8*). Structural modeling studies of the c-Met kinase domain were used to infer that activating mutations interfere with an intrinsic autoinhibition mode (*17*). By stabilizing an active conformation or destabilizing an autoinhibited conformation, the oncogenic mutations promote enhanced kinase activity.

Through the detailed kinetic characterization of highly purified c-Met, we reveal that it is a very efficient catalyst. Studies of the c-Met oncogenic mutant proteins demonstrate that the activation rate is highly dependent on the basal enzymatic activity and has profound effects on the time course of the acquisition of full enzymatic activity upon autophosphorylation. A model is put forth to explain the behavior and provide insight into how a RTK responsiveness can be matched to meet a biological need. Finally, highly specific c-Met inhibitors currently in development [e.g., PF-02341066 (*20*, *21*) and PF-04217903] were biochemically characterized. While PF-02341066 was shown to achieve a very high degree of kinase selectivity (*21*), PF-04217903 demonstrates exquisite kinase selectivity. Inhibition studies of the c-Met mutants show that PF-04217903 is more susceptible to oncogenic mutations that attenuate potency than PF-02341066. For kinases subject to active site mutations, these studies show that inhibitor design may need to balance overall kinase selectivity with the ability to inhibit multiple mutant forms of the kinase (penetrance).

MATERIALS AND METHODS

Materials. [γ-^{32}P]ATP was purchased from GE Healthcare Bio-Sciences (Piscataway, NJ). GF/B glass fiber filterplates and Microscint-20 scintillant were purchased from Packard. The following reagents were purchased from the Sigma-Aldrich (St. Louis, MO): poly(Glu_4Tyr), dephosphorylated α-casein, lactate dehydrogenase, pyruvate kinase, phosphoenolpyruvate, HEPES, MES, NaCl, DTT, $MgCl_2$, ATP, and NADH. Met2 peptide (Ac-ARDMYDKEYYSVHNK) was synthesized on an ABI 433A peptide synthesizer by standard methods and purified to >95% purity by HPLC.

Cloning and Mutagenesis. The cDNA of the human c-Met catalytic domain (residues 1051−1348) was amplified by PCR from human liver Marathon-Ready cDNA (Clontech, Palo Alto, CA) using a forward primer (5′-GATCCCATGGTCCACATTGACCTCAGTGCTC-3′) and a reverse primer (5′-CTAGAAGCTTCTAGTGCTCCCCAATGAAAGTAGAGAAGAT-3′). The cDNA was then subcloned into a modified pFastBac1 expression vector (Invitrogen Inc., Carlsbad, CA) containing an *Nco*I site (pFastBacNcoI). To produce histidine-tagged c-Met, the human c-Met gene comprising the catalytic kinase domain (residues 1051−1348) was cloned into a modified pFastBac1 vector. A noncleavable C-terminal seven-His tag was introduced during cloning. Protein expression was carried out in Sf9 cells at 27 °C in 20 L Wave BioReactors with ESF-921 protein-free medium (Expression Systems). Cells were harvested 48 h after infection. All c-Met mutants were created using a site-directed mutagenesis kit (Stratagene, San Diego, CA) and verified by DNA sequencing.

Expression and Purification. All cDNAs encoding the wild-type and mutant c-Met kinase domains were subcloned or made in the pFastbacNcoI vector. The recombinant baculovirus was generated using the Bac-to-Bac baculovirus expression system (Invitrogen Inc.) and amplified to a level of $1-5 \times 10^8$ PFU/mL in Sf9 insect cells. The recombinant c-Met kinase domain and its mutants were expressed in a 20 L bioreactor by transfecting Sf9 cells with the recombinant baculovirus at a MOI of 5 at 27 °C for 48 h. The cells were harvested by centrifugation at 3000 rpm for 20 min, and the cell pellet was stored at −80 °C.

Untagged c-Met was purified through six chromatography steps. All purification steps were performed at 4 °C. Cell pellets were resuspended in 4 volumes of buffer A [50 mM Tris-HCl (pH 7.8), 150 mM NaCl, 5 mM DTT, and 10% glycerol] supplemented with Protease Inhibitor Cocktail (Sigma) and passed through a microfluidizer (Microfluidics Corp., Newton, MA). The lysate was clarified by ultracentrifugation at 100000*g* and 4 °C for 45 min (Beckman Optima LE-80K ultracentrifuge). The supernatant was passed through a Q-FF Sepharose column, and the flow-through was loaded onto a G-25 column (Pharmacia XK50/60, 1000 mL) equilibrated in buffer B [50 mM MES (pH 6.5), 150 mM NaCl, and 10% glycerol]. Peak fractions from the G-25 column were pooled and applied to a heparin-Sepharose column (Pharmacia XK 26/20) equilibrated in buffer B. Proteins were eluted from the column with a linear salt gradient from

150 to 600 mM NaCl. Fractions containing the recombinant c-Met kinase domain were pooled together, adjusted to 0.6 M ammonium sulfate, stirred at 4 °C for 30 min, and applied to a phenyl-Sepharose column (Pharmacia XK 16/20) equilibrated in buffer C [50 mM MES (pH 6.5), 0.6 M $(NH_4)_2SO_4$, and 3 mM DTT]. The protein was eluted with a linear gradient from 100% buffer C to 100% buffer D [50 mM MES (pH 6.5), 50 mM NaCl, and 3 mM DTT]. Fractions containing the recombinant c-Met kinase domain were pooled and dialyzed against 4 L of buffer E [50 mM MES (pH 6.5), 50 mM NaCl, 10% glycerol, and 3 mM DTT] at 4 °C overnight. The dialyzed solution was then loaded onto a mono S HR 10/10 column in an FPLC system from GE Healthcare Bio-Sciences, washed, and eluted with a linear salt gradient from 50 to 300 mM NaCl. Fractions containing c-Met proteins were pooled, concentrated, and applied to a Superdex 75 HiLoad 16/60 column from GE Healthcare Bio-Sciences equilibrated in 25 mM HEPES (pH 7.5), 150 mM NaCl, 3 mM DTT, and 10% glycerol. The c-Met kinase domain was purified to more than 95% purity as determined by SDS−PAGE. The protein was flash-frozen and stored at −80 °C. The protein concentration was determined using the BCA assay with BSA as the standard.

His-tagged c-Met proteins were purified in a four-chromatography step procedure. All procedures were performed at 4 °C. Frozen cell pellets were resuspended in buffer A [25 mM Tris-HCl (pH 8.0), 150 mM NaCl, 20 mM imidazole, 10% glycerol, 5 mM DTT, and EDTA free protease inhibitor tablets] (Roche Applied Science). Cells were lysed by being passed through a microfluidizer (Microfluidics Corp.) and clarified via ultracentrifugation (Beckman L8-M) at 125171*g* for 45 min. Clarified lysate was passed over a Q HP-Sepharose (GE Healthcare Bio-Sciences). The flow-through fraction was adjusted to pH 8.5 and loaded onto a 20 mL Ni-NTA column (Qiagen, Valencia, CA), washed extensively and step eluted with buffer B [25 mM Tris-HCl (pH 7.5), 150 mM NaCl, 200 mM imidazole, 10% glycerol, and 5 mM DTT]. c-Met eluted from the nickel columnn was dialyzed overnight at 4 °C against 4 L of buffer C [25 mM MES (pH 6.0), 50 mM NaCl, 10% glycerol, and 50 mM DTT]. Dialyzed c-Met was clarified by either filtering or centrifugation and applied to a Source 15S column, washed thoroughly, and eluted with a linear gradient from 50 to 300 mM NaCl. c-Met-containing fractions were dialyzed overnight at 4 °C against 4 L of buffer D [25 mM HEPES (pH 7.5), 300 mM NaCl, 10% glycerol, and 10 mM DTT], concentrated, and loaded onto a HiLoad 26/60 Superdex-75 column (GE Healthcare Bio-Sciences) equilibrated in the same buffer. c-Met-containing fractions were pooled, concentrated to 8−13 mg/mL, flash-frozen in liquid nitrogen, and stored at −80 °C.

Enzymatic Assays. A coupled enzymatic assay format was used to measure both c-Met and phospho-c-Met (p-c-Met) activities which has been described for other kinases (*22*). The kinase-catalyzed production of ADP from ATP that accompanies transfer of phosphate to the random copolymer poly (Glu_4Tyr) or Met2 peptide substrate was coupled to the oxidation of NADH through the sequential actions of pyruvate kinase (PK) and lactate dehydrogenase (LDH). Conversion of NADH to NAD^+ was monitored by the decrease in absorbance at 340 nm (ε = 6.22 cm^{-1} mM^{-1}) using a Beckman DU650 spectrophotometer. A typical reaction solution contained 1 mM phosphoenolpyruvate, 0.24 mM NADH, 20 mM $MgCl_2$, 5 mM DTT, poly(Glu_4Tyr), ATP, 15 units/mL PK, and 15 units/mL LDH in 100 mM HEPES (pH 7.5). The ATP concentration was varied from 0.5 to 2000 μM, and that of poly(Glu_4Tyr) was varied from 0.5 to 20 mg/mL. The conversion of poly(Glu_4Tyr) utilized the MW of the minimal unit that contained a tyrosine residue: Glu_4Tyr, MW = 679.66. For some assays, the Met2 peptide (0−4 mM) was used as a peptide substrate. The Met2 peptide (Ac-ARDMYDKEYYSVHNK) was based on the c-Met activation loop sequence (DFGL*ARDMYDKEYYSVHNKT*-GAKLPVKWMALE). Assays using the Met2 peptide were initiated with the addition of 12 nM phosphorylated c-Met or 125 nM unphosphorylated c-Met. Inhibition studies were performed as described above with the following exceptions: 0.075 mM ATP (p-c-Met) and 0.375 mM ATP (c-Met). The inhibitors were shown to be ATP-competitive from kinetic and crystallographic studies. Data were fit to the equation for competitive inhibition by the method of nonlinear least-squares (GraphPad Prism, GraphPad Software, San Diego, CA).

A second assay format was used to monitor the phosphorylation of a protein substrate. This simple radioactive assay was used to monitor the transfer of phosphate from [γ-^{32}P]ATP to α-casein (*22*, *23*). The filtermate assay format measured the capture of TCA-precipitated ^{32}P-phosphorylated proteins on glass fiber filter plates in a 96-well format. Typical assay conditions for measuring inhibition were established: 27.5 nM p-c-Met, 0.075 mM ATP, 0.0109 mM α-casein, 0.5 μCi of [γ-^{32}P]ATP, 20 mM $MgCl_2$, 2 mM DTT, 100 mM HEPES (pH 7.5), 0.10 mL reaction mixtures, room temperature, 30 min incubation time. These conditions delivered a signal-to-background ratio greater than 20.

The K_i and $K_{m,ATP}$ values for some of the c-Met variants were also determined by a sensitive Omnia continuous fluorometric assay (Invitrogen Inc.) using a tyrosine phosphoacceptor peptide modified by the chelation-enhanced sulfonamide-oxine fluorophore (cSx), coupled with a cysteine residue (*24*). The experimental conditions were similar to the coupled enzymatic assay conditions except the phosphoacceptor was the peptide Ac-EEEEYI(cSx)-IV-NH_2 (Invitrogen Inc.), 2 μM, and 10-fold less c-Met was required. Phosphopeptide formation was monitored in 50 μL volumes in 96-well plates using a Tecan Safire microplate reader with wavelength settings of 360 nm for excitation and 485 nm for emission.

c-Met Autophosphorylation. To achieve high-specific activity phospho-c-Met, large-scale autophosphorylation reactions were performed at high c-Met concentrations, high ATP concentrations, and low temperatures. Typical autophosphorylation reactions for producing maximally active p-c-Met were performed at 4 °C for 4 h with the following components: 10 μM c-Met, 100 mM HEPES (pH 7.5), 20 mM $MgCl_2$, 4 mM ATP, and 2 mM DTT. At fixed time points in the autophosphorylation reaction, the extent of autophosphorylation was measured for enhancement of kinase activity using the coupled enzymatic assay with 2 mM ATP and a variable level of poly(Glu_4Tyr) (0, 0.38, 0.76, 1.5, 3, and 6 mg/mL). The extent of autophosphorylation was also measured by IEF gel electrophoresis analysis (5 μg of protein/time point). Finally, mass spectrometry was used to identify the sites of incorporation of phosphate into c-Met.

Mass Spectrometry. (i) Proteolysis Experiments. Unphosphorylated and phosphorylated c-Met samples were digested by trypsin (100 ng) overnight in a 100 mM ammonium bicarbonate/30% acetonitrile/3 mM Tris-HCl buffer (pH 8) at 37 °C. The tryptic peptides were extracted out of the IEF gels using 50% acetonitrile and 0.1% TFA, concentrated to 10 μL, and subjected to MALDI-TOF and nano-ESI-MS.

(ii) MALDI-MS Analysis. All MALDI-MS analyses were performed in a Voyager-Elite time-of-flight mass spectrometer with delayed extraction (PerSeptive Biosystems, Inc., Framingham, MA). A volume of 1 μL of digested protein was placed directly on the MALDI analysis plate, mixed with 1 μL of matrix (α-cyano-4-hydroxycinnamic acid) in a saturated solution of acetonitrile and water (50:50, v/v) with 0.1% (w/w) TFA, and inserted into the MALDI ionization source for analysis. Samples were irradiated with a nitrogen laser (Laser Science Inc.) operated at 337 nm. The laser beam was attenuated by a neutral density filter onto the sample target. Ions produced by laser desorption were typically energetically stabilized during a delayed extraction period of 150 ns and were then accelerated through the time-of-flight mass analyzer with a potential of 20 kV. Spectra used for analysis were typically an average of 128 laser pulses.

(iii) Nano-ESI-MS. MS/MS analyses were performed on a triple quadrupole mass spectrometer (PE Sciex API III) modified with a nano-ESI source from Protana A/S. The ESI voltage was set at 850 V, and the orifice settings were maintained at 100 V. A curtain gas of ultrapure nitrogen was pumped into the interface at a rate of 0.6 L/min to aid evaporation of solvent droplets and to prevent particulate matter from entering the analyzer. For the precursor ion scan experiment, 3 μL of digested protein was mixed with 3 μL of a 25 mM ammonia solution and 3 μL of methanol (pH 9). For the product ion scan experiment, 3 μL of digested protein was mixed with 7 μL of methanol and 0.5 μL of formic acid. A 4 μL aliquot was loaded into a palladium-coated borosilicate glass capillary and injected into the mass spectrometer. Precursor ion scanning was used to generate spectra of its precursors (or "parent" ions) of the phosphate fragment at m/z 79. A product ion scan was also used to obtain the sequence information of phosphopeptides.

Cellular c-Met Phosphorylation ELISA. Cellular assay procedures were similar to those reported previously (*21*). NIH-3T3 cells were engineered to express human wild-type c-Met or its mutated variants, including c-Met-V1092I, c-Met-H1094R, c-Met-Y1230C, and c-Met-M1250T, and T47D breast carcinoma cells engineered to express human wild-type c-Met or its mutant variant c-Met Y1235D were donated by M. DiRenzo (University of Torino Medical School, Candiolo, Italy). All cells were cultured in the recommended media and serum concentrations, and unless otherwise indicated, cell culture reagents were obtained from Life Technologies, Inc. (Gaithersburg, MD). Cells were maintained at 37 °C in a humidified atmosphere with 5−10% CO_2 and maintained using standard cell culture techniques.

Cells were seeded in 96-well plates in growth medium [medium supplemented with 10% fetal bovine serum (FBS)] and cultured overnight at 37 °C. On the second day of the assay, the growth medium was replaced with serum-free medium (with 0.04% BSA). Serial dilutions of compounds were performed; appropriate controls or designated concentrations of the compounds were added to each well, and cells were incubated at 37 °C for 1 h. Then 40 ng/mL HGF was added to the cells for 20 min. The cells were washed once with HBSS supplemented with 1 mM Na_3VO_4, and protein lysates were generated from cells using lysis buffer (Cell Signaling Technologies, Boston, MA). Phosphorylation of c-Met was assessed by an ELISA method utilizing capture antibodies specific for c-Met and a detection antibody specific for phosphorylated tyrosine residues. Antibody-coated plates were incubated in the presence of protein lysates at 4 °C overnight and washed with 1% Tween 20 in PBS seven times. HRP−PY20 (horseradish peroxidase-conjugated anti-phosphotyrosine, from Santa Cruz Biotechnology, Santa Cruz, CA) was diluted 1:500 in blocking buffer (Pierce, Rockford, IL) and added to each plate for 30 min. Plates were then washed again, and TMB peroxidase substrate (Bio-Rad Laboratories, Hercules, CA) was added to initiate the HRP-dependent colorimetric reaction and the reaction stopped by addition of 0.09 N H_2SO_4. ELISA end points were the absorbance measured at 450 nm using a spectrophotometer. IC_{50} values were calculated by concentration−response curve fitting utilizing a Microsoft Excel-based four-parameter analytical method.

Differential Scanning Fluorimetry. Melting temperatures were determined on a FluoDia T70 differential scanning fluorimeter (Photon Technology International, Inc., Birmingham, NJ). Reaction mixtures were 50 μL in volume and contained 1.5 μM c-Met, 5 μM inhibitor, and 2% DMSO in buffer containing 25 mM HEPES (pH 7.5), 300 mM NaCl, 10% glycerol, and 2 mM TCEP. Protein and compounds were complexed for 30 min at room temperature followed by addition of a fluorophore. Reaction solutions were mixed and layered with 100 μL of mineral oil (USB Corp., Cleveland, OH) in MJ(96) HSP-9601 plates (MJ Research, Cambridge, MA) before the plates were placed into the machine. The thermal unfolding of c-Met proteins was monitored as an increase in the magnitude of the fluorescence signal over a temperature range of 25−75 °C increasing 1 °C/min using SYPRO-Orange (Invitrogen Inc.) as the fluorophore. Melting temperature (T_m) values were calculated using software developed in-house. In short, a modified script plots the absorbance as a function of time, calculates the "half-melting time", and extrapolates this measurement (in seconds) into melting temperature (degrees Celsius) based on the linear regression of the time versus temperature data from the instrument.

Surface Plasmon Resonance Assay. A surface plasmon resonance (SPR) assay was used to determine binding affinities (K_d) and off rates for PF-02341066 and PF-04217903 binding to c-Met on a Biacore 3000 instrument (GE Healthcare Bio-Sciences). c-Met protein was diluted into 10 mM sodium acetate (pH 5.5) and immobilized to a Biacore CM5 sensor chip using a modified amine coupling procedure: 7 min NHS/EDC activation, 10 min protein contact time, 2 min NHS/EDC stabilization step, and 7 min ethanolamine-HCl deactivation. Increasing concentrations of compound (7.8, 15.6, 31.2, 62.5, 125, 250, 500, and 1000 nM) were injected using Kinject mode (1 min association and 5 min dissociation) at a rate of 50 μL/min in assay buffer [25 mM HEPES (pH 7.5), 150 mM NaCl, 10 mM $MgCl_2$, 0.2 mM DTT, 0.005% polysorbate 20 (Tween 20), and 2% DMSO]. There was no surface regeneration between the concentrations because an effective solution that did not adversely affect the activity of the immobilized c-Met could not be found. The sensorgram was fit to a 1:1 Langmuir binding model with mass transport in Scrubber-2 (BioLogic Software Pty Ltd., Campbell, Australia) to determine the binding affinity. The off rates were determined using a 1:1 Langmuir dissociation model analysis (independent of the on rate and binding affinity) for only the 7.8 nM concentration, due to incomplete regeneration of the surface at higher compound concentrations, using Scrubber-2.

RESULTS

Autophosphorylation of c-Met. Essential to meaningful biochemical and crystallographic studies is highly purified and highly active protein. The c-Met catalytic domain was expressed

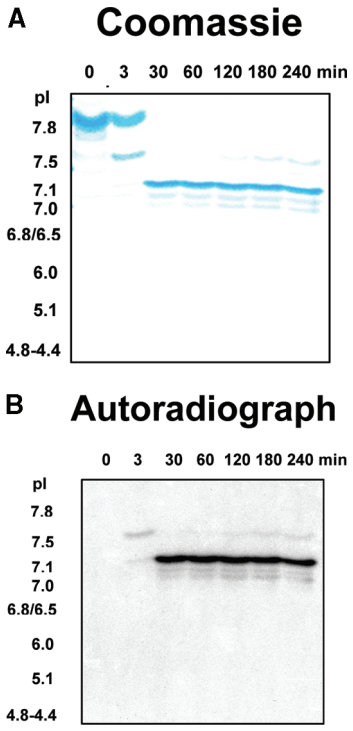

FIGURE 1: Characterization of the time course of the c-Met autophosphorylation reaction. c-Met autophosphorylation proceeds through sequential phosphorylation events. (A) Coomassie-stained isoelectric focusing (IEF) electrophoretic evaluation of a time course (4 °C, 4 mM ATP, 17 μM c-Met) of c-Met autophosphorylation shows that initially, c-Met has a pI of 7.9. The next species formed has a pI of 7.6. Further autophosphorylation shifts c-Met to a third species (pI of 7.2). (B) Autoradiogram of the IEF gel.

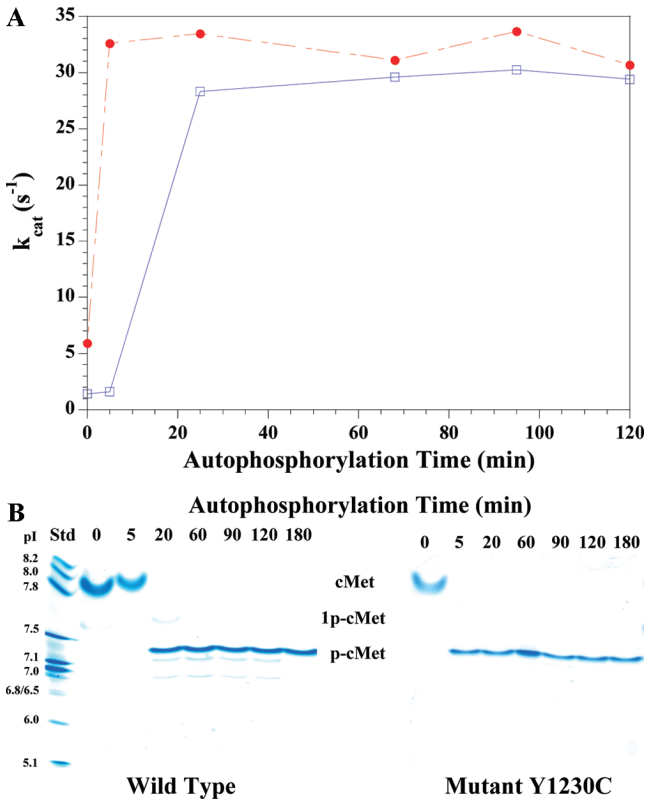

FIGURE 2: Evaluation of the relative rate of autophosphorylation of the c-Met mutant Y1230C compared to wild-type c-Met. c-Met autophosphorylation causes a large increase in catalytic potency (k_{cat}). (A) Time course of autophosphorylation of wild-type (□) and Y1230C mutant c-Met protein (●). (B) Evaluation of the phosphorylation status of wild-type (left) and Y1230C mutant c-Met (right). Reaction mixtures contained 10 μM c-Met and 4 mM ATP, and reactions were carried out at 4 °C.

using a baculoviral expression system and isolated from cell lysates through a purification utilizing six chromatographic steps. c-Met was activated by an autophosphorylation reaction to produce phospho-c-Met (p-c-Met). The extent of the autophosphorylation reaction was monitored by multiple methods: native IEF with both Coomassie staining for protein (Figures 1A and 2B) and [^{32}P]phosphate incorporation by autoradiography (Figure 1B). IEF analysis revealed that the c-Met kinase domain had a pI of 7.9 (Figure 1A). Limited autophosphorylation shifted c-Met to a second species with a pI of 7.6 (Figure 1A,B). Further autophosphorylation shifted c-Met to a third species (pI of 7.2). As such, there appears to be two phosphate transfer events. The catalytic efficiency of the c-Met catalytic domain increased as a function of autophosphorylation time (Figure 2A) and corresponded to changes in phosphorylation state as measured by IEF analysis. In addition, the rate of autophosphorylation was found to be dependent on the concentration of c-Met (data not shown). Although sequential phosphorylation events can be inferred by the IEF analysis, the precise assignment of these sites was not possible.

The determination of the phosphorylation sites and order of phosphate incorporation was investigated by mass spectrometric analysis of samples of c-Met and fully phosphorylated c-Met (p-c-Met). The samples were proteolyzed with trypsin and subjected to MALDI-TOF mass spectrometry. There was one major, doubly phosphorylated peptide identified. This phosphopeptide corresponded to c-Met residues 1233−1240 (SYYSVHNK) which are contained in the c-Met activation loop. Parent ion scans using nano-ESI mass spectrometry confirmed the identified sites. Both the IEF and MS data were consistent with two sequential autophosphorylation reactions on residues Y1234 and Y1235 which were identified previously (*6*). No evidence of the c-Met-mediated autophosphorylation of tyrosine residue 1194 was found.

Kinetic Analysis of c-Met and p-c-Met. The kinetic consequences of the autophosphorylation were investigated by evaluating c-Met and p-c-Met activities in two distinct and complementing assay formats: (1) continuous assay format using a coupled enzymatic assay that measured ADP formation and (2) a discontinuous format that directly measured phosphate incorporation through a radiometric format. Three substrates were evaluated by this method: poly(Glu$_4$Tyr), c-Met activation loop peptide (Met2), and dephosphorylated α-casein. The enzymatic activity of c-Met was linear with respect to enzyme concentration (0−200 nM) at a saturating ATP concentration (1 mM), a saturating poly(Glu$_4$Tyr) concentration (7.4 mM), and a saturating $MgCl_2$ concentration (40 mM). Enzymatic activity was similar in MES and HEPES buffers. At pH 6.8, the k_{cat} values were similar (14.0 s^{-1} in HEPES and 14.3 s^{-1} in MES) as were the poly(Glu$_4$Tyr) K_m values (K_m = 3.4 mM in HEPES, and K_m = 4.1 mM in MES). Enzymatic activities (k_{cat}/K_m values) were determined at saturating ATP concentrations, variable poly(Glu$_4$Tyr) concentrations, and variable HEPES pH values (6.0, 6.8, 7.0, 7.5, and 8.0). The c-Met activity was similar at all pH values as demonstrated by the variation of determined k_{cat}/K_m values from the average value (k_{cat}/K_m = 3820 ± 450 M^{-1} s^{-1}). Maximal enzymatic activity could be

Table 1: Effect of Autophosphorylation on Enhancement of c-Met Steady-State Kinetic Parameters[a]

	unphosphorylated c-Met	p-c-Met
$K_{m,ATP}$ (μM)	373 ± 60	73.7 ± 2.8
$K_{m,poly(Glu_4,Tyr)}$ (μM)	4720 ± 260	3100 ± 570
k_{cat} (s^{-1})	1.02 ± 0.01	31.3 ± 2.0
k_{cat}/K_m (s^{-1} M^{-1})	2730	425000

[a] All kinetic parameters except $K_{m,ATP}$ were determined in the coupled enzymatic assay at 37 °C, saturating ATP concentrations (2 mM), and variable poly(Glu_4,Tyr) concentrations. The $K_{m,ATP}$ was determined at 7.4 mM poly(Glu_4,Tyr) with variable ATP concentrations.

achieved with $MgCl_2$ concentrations greater than 10 mM with the concentration to achieve half-maximal activity determined to be 3 mM. A detailed kinetic analysis of unphosphorylated and fully phosphorylated c-Met was performed with the substrate poly (Glu_4,Tyr) using a coupled enzymatic assay (Table 1). c-Met autophosphorylation resulted in a large, 31-fold increase in k_{cat} (from 1.0 to 31.3 s^{-1}), a 5-fold decrease in $K_{m,ATP}$ (from 373 to 73.7 uM), and a 160-fold increase in k_{cat}/K_m. Fully active c-Met is a potent catalyst with a k_{cat}/K_m of 425000 M^{-1} s^{-1}. As such, autophosphorylation has a profound impact on the catalytic efficiency of c-Met. To confirm the results, a peptide substrate based on the activation loop of c-Met (Met2 peptide) was evaluated. The kinetic analysis of the Met2 peptide was performed with phosphorylated c-Met which was shown to have the following properties: k_{cat} = 3.7 ± 0.6 s^{-1}, $K_{m,ATP}$ = 73.7 ± 2.9 μM, and $K_{m,peptide}$ = 408 ± 116 μM. Parameters differed slightly in a separate experiment conducted using different assay conditions (Table 3). A nearly 100-fold increase in k_{cat} was observed with the Met2 peptide upon enzyme activation. A full-length protein was identified as a substrate (dephosphorylated α-casein) with the K_m value determined to be 28.5 ± 3.5 μM. A second assay format was used to measure the production of ^{32}P-labeled phosphoprotein (dephosphorylated α-casein) as a direct measurement of the phosphate transfer reaction of p-c-Met. The radiometric assay yielded a $K_{m,\ ATP}$ similar to that observed in the coupled, enzymatic reaction (78.6 ± 12.1 μM). The $K_{m,ATP}$ value was found to be essentially independent of assay format and phosphoacceptor. As determined in multiple assays with multiple phosphoacceptor substrates, c-Met autophosphorylation has a profound effect on the kinetic properties of c-Met and transforms it into a very effective catalyst.

Kinetic Characterization of c-Met Mutants. A detailed evaluation of the enzymatic consequences of oncogenic mutations on c-Met catalysis was undertaken. The autophosphorylation time course for c-Met mutant Y1230C was measured in parallel with wild-type c-Met by determining the k_{cat} at a saturating ATP concentration and variable poly(Glu_4Tyr) concentrations (Figure 2a). The basal level of activity of the Y1230C mutant was determined to be 6-fold higher than for the wild type (Table 2). Upon complete autophosphorylation, both Y1230C mutant and wild-type c-Met preparations achieve similar maximal activity (k_{cat} = 32 s^{-1} vs 31 s^{-1}). The kinetic parameters of Y1230C were re-examined with a different substrate and shown to have a similar result (Table 3). The coupled enzymatic assay measures ADP production. To ensure that the Y1230C mutation did not enhance the nonproductive hydrolysis of ATP (ATPase activity), both wild-type and mutant c-Met activity was measured in the absence of poly(Glu_4Tyr) (variable ATP). In the absence of a phosphoacceptor, both wild-type and Y1230C mutant c-Met had

Table 2: Kinetic Evaluation of the Y1230C c-Met Mutation[a]

	unphosphorylated Y1230C c-Met mutant	phosphorylated Y1230C c-Met mutant
$K_{m,ATP}$ (μM)	243 ± 23	110 ± 13
$K_{m,poly(Glu_4,Tyr)}$ (μM)	3840 ± 220	3280 ± 760
k_{cat} (s^{-1})	5.9 ± 1.7	32.2 ± 1.1
k_{cat}/K_m (s^{-1} M^{-1})	24300	293000

[a] All kinetic parameters except $K_{m,ATP}$ were determined in the coupled enzymatic assay at 37 °C, saturating ATP concentrations (2 mM), and variable poly(Glu_4,Tyr) concentrations. The $K_{m,ATP}$ was determined at 7.4 mM poly(Glu_4,Tyr) with variable ATP concentrations.

Table 3: Kinetic Characterization of c-Met Mutant Constructs in both the Unactivated and Activated (Autophosphorylation) States[a]

	k_{cat} (s^{-1})		$K_{m,ATP}$ (μM)	$K_{m,Met2\ peptide}$ (mM)
	unactivated	activated	activated	activated
WT	0.08 ± 0.01	8.4 ± 1.6	96 ± 11	1.4 ± 0.5
H1094R	0.58 ± 0.14	8.5 ± 1.7	118 ± 7	1.1 ± 0.7
L1195V[b]	ND[c]	14.7 ± 4.7	82 ± 4	0.7 ± 0.3
M1131T	0.12 ± 0.03	5.0 ± 2.2	96 ± 8	1.0 ± 0.4
V1220I	0.13 ± 0.10	9.6 ± 3.2	164 ± 16	0.8 ± 0.8
D1228H	0.27 ± 0.05	11.3 ± 3.0	76 ± 3	0.6 ± 0.4
Y1230C	0.79 ± 0.10	12.8 ± 4.1	75 ± 6	1.0 ± 0.4
Y1230H	0.32 ± 0.12	11 ± 6	64 ± 4	1.0 ± 1.2
Y1235D	0.15 ± 0.04	1.5 ± 2.6	55 ± 5	ND[c]

[a] The k_{cat} values were determined in the coupled enzymatic analysis of c-Met processing of the Met2 peptide (0−2 mM) and MgATP (1.5 mM ATP/10 mM $MgCl_2$) at 37 °C. The $K_{m,Met2\ peptide}$ values were determined at a saturating concentration of ATP, and the $K_{m,ATP}$ values were measured at variable ATP concentrations and a constant Met2 peptide concentration (1 mM), except $K_{m,ATP}$ for the Y1235D mutant which was determined by an Omnia fluorometric assay. $K_{m,ATP}$ values for wild-type protein were similar in both assays (data not shown). Errors were generated from the analysis of multiple separate determinations. [b] Isolated as a doubly phosphorylated protein. [c] Values not determined.

the same minimal level of nonproductive ATP hydrolysis (< 2% of the rate with the phosphoacceptor). Next, we examined the phosphorylation time course for Y1230C in parallel with wild-type c-Met by IEF analysis to evaluate phosphorylation events on the protein (Figure 2B). No phosphorylation of the Y1230C mutant was detected in the absence of ATP. The Y1230C mutant autophosphorylation reaction produced similar shifts in pI compared to those of the wild type. The mutation appears to cause a more rapid autophosphorylation reaction as determined by the rapid conversion of unphosphorylated c-Met to a fully phosphorylated form. By different methods, the Y1230C activating mutation caused a higher basal level of activity but did not alter the maximal activity achieved upon autophosphorylation.

The study of oncogenic mutants was expanded to include a larger panel of clinically relevant c-Met mutations. To ensure that the activities of the c-Met mutant proteins were from unphosphorylated forms, all of the purified proteins were characterized by mass spectrometry. Intact mass spectrometric analysis was used to confirm the phosphorylation status of the proteins (data not shown). In all cases except mutant L1195V, the mutant proteins were isolated in the unphosphorylated form. The effect of the c-Met mutations on protein stability as measured by melting temperatures was performed by differential scanning fluorimetry (Table 6). The melting temperatures (T_m) of the wild-type and mutant c-Met proteins were relatively constant (42−43 °C) with one exception (L1195V, 38.9 °C). The con-

sequences of the mutations on catalysis were evaluated through the determination of the kinetic parameters for the different phosphorylation states of c-Met (Table 3). The c-Met k_{cat} values were determined using the c-Met activation loop peptide (Met2) as the phosphoacceptor. All of the mutants, except Y1235D, achieved full activation, comparable to that of wild-type c-Met. This was an interesting result because Y1235 is one of the two tyrosine residues autophosphorylated in the activation loop. When the unactivated mutants were evaluated, Y1230C had the highest basal k_{cat} value (10-fold more active than the wild-type enzyme), and the other mutants were ~2−7-fold more active. It should be noted that mutant L1195V when purified from insect cell lysates was already fully phosphorylated on the activation loop. This may indicate that this mutation confers significant basal activity that accelerates the autophosphorylation rate, but we cannot rule out the possibility that the mutant makes the activation loop a substrate for another kinase found in insect cells. The functional consequences of the mutations on the activation rate were studied by measuring the time course of activation. Analysis of the time course of the acquisition of enzymatic activity (Figure 3) showed markedly different activation profiles for the different mutant proteins. For example, the Y1230C mutation achieved full activation in < 20 min because it achieved the maximal rate (product per time). In contrast, the wild-type c-Met protein remained at the basal level of activity after reaction for 40 min. Three mutant c-Met proteins (M1131T, V1220I, and Y1235D) had activation profiles similar to that of the wild type. These three mutant proteins all had less than 2-fold enhancement of the basal k_{cat} values. The four mutant proteins that had significantly accelerated activation profiles (Y1230C, Y1230H, D1228H, and H1094R) had basal k_{cat} values that were 4−10-fold larger than the wild-type value. As shown in Figure 3, c-Met mutant proteins acquired full enzymatic activity at different rates.

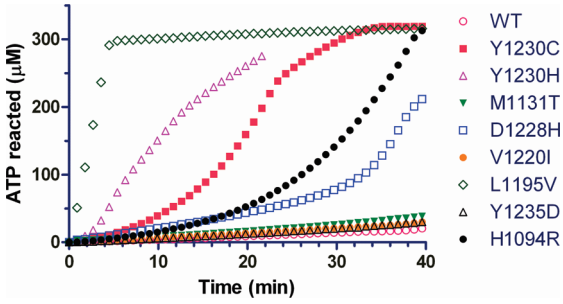

FIGURE 3: c-Met mutant activation time course as measured by phosphorylation of the Met2 peptide. Coupled assay reactions were conducted using 100 nM nonactivated enzyme (except L1195V that was fully phosphorylated), 1.5 mM ATP, and 1 mM Met2 peptide at 37 °C. The maximum ATP consumption was limited by NADH (0.33 mM), the coupling reagent.

Table 4: Biochemical and Cellular Inhibition of Wild-Type c-Met and Oncogenic c-Met Mutants by Inhibitors of Two Different Chemical Series[a]

Compound	Structure	WT (His6-tagged)	WT (un-tagged)	Y1230C	Y1230H	D1228H	M1131T	V1220I	L1195V	H1094R	Y1235D
PF-02341066	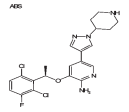	0.0063 ± 0.0013	0.0055 ± 0.0005	0.051 ± 0.005	0.047 ± 0.005	0.064 ± 0.003	0.0042 ± 0.0013	0.017 ± 0.003	0.038 ± 0.004	0.0092 ± 0.0010	0.024 ± 0.009
PF-03386065	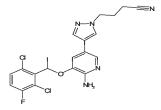	0.049 ± 0.007	0.053 ± 0.006	0.323 ± 0.043	0.336 ± 0.034	0.418 ± 0.035	0.064 ± 0.006	0.154 ± 0.017	0.281 ± 0.037	0.084 ± 0.007	0.136 ± 0.035
PF-03775712	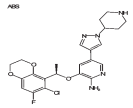	0.016 ± 0.002	0.019 ± 0.002	0.210 ± 0.018	0.211 ± 0.037	0.282 ± 0.029	0.039 ± 0.013	0.057 ± 0.008	0.138 ± 0.012	0.025 ± 0.001	0.050 ± 0.005
PF-04217903	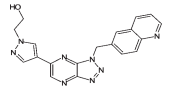	0.0065 ± 0.0010	0.0074 ± 0.0016	9.4 ± 1.3	3.9 ± 0.5	>10	0.013 ± 0.002	0.039 ± 0.009	0.31 ± 0.03	0.0026 ± 0.0013	0.044 ± 0.009
PF-04254644	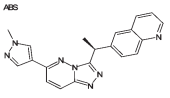	0.014 ± 0.002	0.017 ± 0.002	>10	8.9 ± 1.2	>2.5	0.059 ± 0.002	0.093 ± 0.009	0.692 ± 0.084	0.0080 ± 0.0016	0.049 ± 0.003
PF-04297248	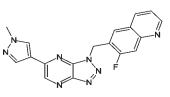	0.0039 ± 0.0010	0.019 ± 0.003	>10	4.3 ± 0.2	>10	0.017 ± 0.002	0.036 ± 0.004	0.245 ± 0.038	0.0090 ± 0.0010	0.066 ± 0.017
PF-04327458	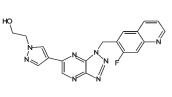	0.0030 ± 0.0005	0.0031 ± 0.0009	10 ± 1	3.5 ± 0.5	>10	0.0082 ± 0.0013	0.020 ± 0.003	0.157 ± 0.025	0.0028 ± 0.0006	0.049 ± 0.003

[a] All of the proteins had C-terminal His_6 tags except wild-type c-Met, for which both tagged and untagged versions were evaluated. K_i values ± the standard error of the mean were determined from fits to the Morrison quadratic equation using data generated by a coupled spectrophotometric assay at 37 °C with a 30 min pre-incubation of enzyme with compounds prior to addition of ATP. ATP $K_{m,app}$ values ± the standard error of the mean are shown for assays conducted in duplicate. The K_i for the Y1235D mutant was determined by an Omnia fluorometric assay. K_i values for the wild-type protein were similar in both assays (data not shown).

Table 5: Inhibitor Potency in Cellular Assays[a]

c-Met mutation	cell line	IC_{50} (nM) PF-02341066[b]	PF-04254644	PF-04297248	PF-04217903
endogenous human WT c-Met	A549 human lung carcinoma	8.6 ± 2	5.6 ± 1.3	0.9 ± 0.1	4.8 ± 1.6
endogenous c-Met-R988C	H69 human lung carcinoma	11.4	6.4 ± 2.0	1.7 ± 0.3	6.4 ± 1.8
endogenous c-Met-T1010I	HOP-92 human lung carcinoma	15	8.1 ± 0.2	1.2	6.7 ± 0.2
engineered human WT c-Met	3T3-c-Met WT	12.6 ± 3.4	13.4 ± 1.1	1.7	16.9 ± 3.0
engineered c-Met-V1092I	3T3-c-Met-V1021I	18.7	9	2.5	16.0 ± 1.5
engineered c-Met-H1094R	3T3-c-Met-H1094R	2.2 ± 0.3	1.6	< 1	3.1
engineered c-Met-Y1230C	3T3-c-Met-Y1230C	127 ± 29	> 10000	> 10000	> 10000
engineered c-Met-M1250T	3T3-c-Met-M1250T	15 ± 3	18.0 ± 2.4	2.8	24 ± 16
engineered human WT c-Met	T47D-c-Met WT	14.7	5.8 ± 2.4	1.3 ± 0.2	5.8 ± 1.4
engineered c-Met-Y1235D	T47D-c-Met-Y1235D	104	153 ± 35	44 ± 8	142 ± 19

[a] Values were derived by multiple independent experiments except for values without errors associated with the IC_{50} value. [b] Most data for PF-02341066 were previously reported (*21*).

Inhibition of c-Met and Phospho-c-Met by Small Molecule Inhibitors. We utilized a series of small molecule inhibitors to further study the topography of an active site. Inhibition of c-Met and p-c-Met was first evaluated with a well-characterized, nonspecific kinase inhibitor, staurosporine. The inhibition constants (K_i) of staurosporine were measured to be 260 ± 16 nM for unactivated c-Met and 132 ± 6 nM for activated c-Met. Two classes of optimized c-Met inhibitors currently in development were used to assess potency and selectivity toward c-Met and its clinically relevant mutants. PF-02341066 is the prototype inhibitor from the 3-benzyloxy-2-aminopyridine (BOAP) chemical series, while PF-04217903 is a prototypical inhibitor from the triazolopyrazine (TAP) chemical series (Table 4). The inhibitors were evaluated in biochemical assays (Table 4) and cellular assays (Table 5) that measured the activity of c-Met and its oncogenic mutants. Biochemically, both classes of inhibitors were very potent inhibitors of c-Met with K_i values ranging from 3 to 53 nM. The potencies were found to be independent of whether there was a hexahistidine affinity tag present on the protein (Table 4). Surface plasmon resonance studies of the binding of PF-02341066 (K_d = 4.3 nM; $t_{1/2}$ = 400 s) and PF-04217903 (K_d = 4.5 nM; $t_{1/2}$ = 180 s) confirmed the enzymatic inhibition data (both K_i values of 6−7 nM) but showed a modest difference in residence time in the c-Met active site (400 s vs 180 s). Differential scanning fluorimetry was used to confirm binding. Large increases in the melting temperatures (14−16 °C) were observed for c-Met upon binding of either PF-02341066 or PF-04217903. By multiple measures, both chemical series (BOAP and TAP) are potent inhibitors of c-Met.

The kinase selectivity of both chemical series was assessed by profiling the biochemical potency against a panel of kinase assays. Previously reported studies of PF-02341066 have shown it to be highly selective (*21*). In this study, we report that PF-04217903 is also highly selective for c-Met. PF-04217903 was evaluated against multiple kinase selectivity screening panels: Invitrogen Inc. (125 kinases), Millipore/Upstate Ltd. (105 kinases), University of Dundee (51 kinases), and Pfizer in-house (48 kinases) (Supporting Information). On the basis of the percent inhibition or IC_{50} values generated from each of these screens, PF-04217903 was estimated to be > 1000-fold selective for c-Met compared with each of the other kinases included in these collective screening assays. Therefore, PF-04217903 demonstrated exquisite selectivity for c-Met compared with a diverse panel of 208 kinases representing ~40% of the known kinome. PF-04217903 and PF-02341066 represent unique examples of ATP-competitive kinase inhibitors that achieve very high kinase selectivity profiles.

Table 6: Biophysical Evaluation of Wild-Type and Mutant c-Met Proteins by Differential Scanning Fluorimetry To Determine Melting Temperatures (T_m)[a]

	c-Met T_m (°C) no inhibitor	PF-2341066	differential	PF-4217903	differential
WT	42.9	57.4	14.5	58.8	15.9
Y1230C	42.0	50.1	8.1	44.1	2.1
M1131T	42.8	ND[b]	ND[b]	ND[b]	ND[b]
D1228H	43.1	50.5	7.4	44.2	1.1
V1220I	43.7	57.0	13.3	57.7	14.0
L1195V	38.9	50.8	11.9	50.5	11.6
Y1235D	41.9	53.5	11.7	53.7	11.8
H1094R	42.3	57.3	15.0	59.3	17.0
Y1230H	42.0	51.8	9.8	46.4	4.4

[a] All c-Met proteins except L1195V had similar T_m values. The differential temperature refers to the difference between the apoprotein T_m and the T_m of the protein−inhibitor complex. The magnitude of the differential T_m value correlated with the determined inhibition constants (K_i). [b] Not determined.

Inhibition of the c-Met oncogenic mutants was evaluated in both biochemical and cellular contexts. The potency values of seven members of two chemical series were determined for eight c-Met oncogenic mutations (Tables 4 and 5). Biochemically, the BOAP chemical series was equally potent (< 3-fold difference) toward M1131T, V1220I, H1094R, and Y1235D mutations and had a significant potency loss (~10-fold) toward the following mutations: Y1230C, Y1230H, D1228H, and L1195V. This pattern of potency retention or loss was conserved across the three tested molecules. In the TAP series, a similar overall pattern of selectivity was observed except when there were potency shifts, they were substantially larger (for Y1230 and D1228 > 1000-fold) than those observed for the PF-02341066 chemical series. The thermal stability of the mutants with and without inhibitors was evaluated using differential scanning fluorimetry (DSF) (*25*, *26*) (Table 6). The amount of T_m shift upon inhibitor binding was well-correlated with the measured biochemical and cellular potency (Tables 4 and 5). For example, the mutant proteins that did not perturb compound binding (e.g., H1094R) underwent a large increase in T_m (15−17 °C) upon binding of PF-02341066 and PF-04217903. Mutant c-Met proteins that exhibited higher K_i values (e.g., Y1230C) had proportionally smaller T_m shifts (e.g., 2−8 °C). The same trend in differential

potency shifts for the PF-02341066 and PF-04217903 chemical series was observed in the subset of c-Met mutations profiled in a cellular context (Table 5). The pattern of potency, also observed with other compounds from the two chemical series (Tables 4 and 5), indicates that these two chemical series are making differential and unique binding interactions with c-Met.

DISCUSSION

Kinetic Analysis of c-Met and p-c-Met. Receptor autophosphorylation is an essential event in cellular signal transduction pathways with multiple functions in vivo, including activation of the catalytic domain and creation of recruitment sites for downstream signaling molecules. Kinetic analysis of unphosphorylated and autophosphorylated c-Met was undertaken to characterize the overall effect of autophosphorylation on the effectiveness and efficiency of c-Met as a catalyst. Autophosphorylation was initially reported to effect a few-fold V_{max} enhancement of c-Met (*5*). More recent kinetic studies of the recombinantly expressed cytoplasmic domain of c-Met have reported that the k_{cat} was only 0.0095 s^{-1} (k_{cat}/K_m = 140 s^{-1} M^{-1}) (*11*). In contrast, the current study shows that highly purified, fully activated c-Met is a highly efficient catalyst (k_{cat}/K_m = 425000 s^{-1} M^{-1}). The K_m of ATP for the activated receptor was similar to the reported studies: immunoprecipitated c-Met from cells ($K_{m,ATP}$ = 36 μM) (*3*) and recombinantly expressed cytoplasmic domain of c-Met ($K_{m,ATP}$ = 70.4 μM) (*8*). The similarity of the $K_{m,ATP}$ values to those from the previous studies and the large difference in the observed catalytic power could be due to fractions of the c-Met that is in a conformation appropriate for catalysis. Contrary to previously published results, c-Met is a highly effective catalyst which undergoes a large enhancement in catalytic power in the autophosphorylation process. This result is not observed for all RTKs. Autophosphorylation of a subset of kinases produces small enhancements in catalytic power, while large increases are observed for other kinases. For example, the VEGFR2 receptor tyrosine kinase has similar turnover numbers for both unphosphorylated (k_{cat} = 5 s^{-1}) and autophosphorylated (k_{cat} = 12 s^{-1}) forms with the k_{cat}/K_m increasing 10-fold (*27*). An example of a RTK that has a profound change in catalytic efficiency is Tie2 which undergoes a 460-fold increase in k_{cat}/K_m (*22*). Alternatively, autophosphorylation of some RTKs such as EGFR has been shown to have no effect on receptor activation (*28*). c-Met is a receptor tyrosine kinase with its activity highly dependent on the phosphorylation state of the catalytic domain.

This study shows that the c-Met activation time course is sensitive to oncogenic mutations in the kinase domain. The Y1230C mutation was shown to enhance the c-Met activation rates. The simplest explanation for the faster activation of the Y1230C mutation is that it possesses higher intrinsic catalytic activity (6−10-fold increase in k_{cat} values) which causes a more rapid autophosphorylation reaction. The mutants appear to alter c-Met k_{cat} but not K_m values. Care was taken to ensure that the starting conditions were truly unphosphorylated by using intact mass spectrometric analysis, but the possibility that a differential low level of phosphorylation not detected by mass spectrometry is present remains. From the time course of activation (Figure 3), one can see that small enhancements in basal activity can have large effects on the acquisition of full catalytic activity. Biophysical studies were used to further understand the role of the mutations on c-Met. The differential scanning fluorimetry studies showed that the oncogenic mutations do not have a large effect on protein stability. The c-Met T_m values derived in this study are in line with the range of T_m values found in the panel of 221 proteins (*26*). Taken together, the biochemical and biophysical data suggest that mutations may affect local conformational changes in the catalytic and inhibitor binding sites without causing a large overall protein conformational change.

A Model for c-Met Activation. Activating mutations of c-Met have been shown to autophosphorylate faster than the wild type yet achieve the same maximum activity (*8*). We show that the increased autophosphorylation rate is based in the enhancement in k_{cat} which is a measure of catalytic effectiveness. There was little effect on K_m for any substrate which indicates that the effects are not substrate-specific. A computational model of c-Met regulation has recently been put forth to predict cellular responses (*10*). The model predicts a direct correlation between the c-Met k_{cat} for autophosphorylation and accumulation of phosphorylated c-Met. The model used the preexisting data that reported a 10-fold enhancement in kinase activity between the c-Met basal and activated states. Highly purified and activated c-Met used in this study shows that the activation is more profound, 160-fold enhancement in kinase activity. A refinement of the model based on new kinetic data is proposed to describe a geometric progression of activity in the autophosphorylation process that is sensitive to both basal and maximal activities. The activation process can be separated into initiation of activation from an unactivated state and subsequent acquisition of activity with a mixture of both enzymatic activities (basal and activated forms). The initiation of the activation process from the unactivated state is an intermolecular, bimolecular process which is highly dependent on the kinase concentration. Enhancements in the basal kinase activity increase the likelihood that an intermolecular encounter is productive and results in the phosphorylation of an activation loop residue. The subsequent acquisition of activity is more complex because it encompasses both reactions of kinase molecules with basal activity and elevated enzymatic activity. This acquisition process can be considered in terms of a geometric progression. A geometric progression (a, ar, ar^2, ar^3, ...) has a scalar factor (a) and a common ratio factor (r). The common ratio of the progression of c-Met activation is the catalytic activity of the fully activated c-Met. The progression is geometric because each activated (phosphorylated) c-Met molecule will phosphorylate more unactivated c-Met molecules than c-Met with basal activity. In addition, the difference between the catalytic capacities of the two activation states has a direct impact on the activation time course because it defines the steepness of the response curve. As such, the sensitivity of the biological response can be based, in part, on the absolute activities of the activated and inactivated forms and the magnitude of the differential in catalytic power between the states. These attributes of the autophosphorylation reaction can contribute to the switchlike behavior that allows for rapid accumulation of enzymatic activity. In addition, this model predicts that the RTK response can be matched to the biology it impacts by alterations in basal and fully active catalytic parameters. For some receptor tyrosine kinases, a fast accumulation of active enzyme may be desirable so a larger enhancement in catalytic activity would allow for a more sensitive activation time course. Conversely, a small enhancement in catalytic activity upon autophosphorylation could yield a different activation time course. Many elegant computational studies of bistable networks dependent on kinase phosphorylation have been previously

described (*29*−*31*), but the described networks typically model unphosphorylated kinase as inactive, not active as shown for c-Met. The original modeling of autophosphorylation by Lisman (*31*) can be extended to receptor tyrosine kinases if the initiating kinase is actually the RTK with basal activity. Nonetheless, the data for c-Met show that it is sensitive to small enhancements in basal activity which are translated to a much more rapid activation time course by the large differential between activated and unactivated states.

Evaluation of c-Met Inhibitors. Both nonspecific and highly specific kinase inhibitors were used to characterize binding interactions with c-Met. As expected, the general kinase inhibitor staurosporine was potent, but not selective for different phosphorylation states of c-Met. The K_i values determined in this study are consistent with the published values (150−190 nM) (*9*) which indicates that the biochemical potency values are properties of the protein and not specific to assay conditions. Highly optimized kinase inhibitors from multiple chemical series currently in clinical trials achieved high levels of inhibitory potency. Biophysical studies using either perturbation of melting temperatures or surface plasmon resonance confirmed the inhibitor potencies. The magnitudes of the T_m shifts observed with the c-Met inhibitors are consistent with the observed inhibition constants derived from kinetic studies because the observed 14−16 °C T_m shifts could be expected for inhibitors with biochemical potency (K_i) values ranging from 5 to 10 nM. Melting temperature shifts of 4 °C have been reported to translate to IC_{50} values of < 1 μM (*26*). Interestingly, the biophysical interactions defined in SPR studies show that there was a significant 2-fold difference in the residence time ($t_{1/2}$) even though the measured K_d values were nearly identical. By all measures, the optimized c-Met inhibitors are highly potent molecules.

Kinase selectivity of inhibitors can be defined at multiple levels: (1) relative to other kinases, (2) between different conformations of the same enzyme (activated vs unactivated), and (3) among different mutants of the same enzyme. Previously reported studies of PF-02341066 have shown it to be highly selective (*21*). More than 90% of the 120 kinases tested showed a 100-fold selectivity for c-Met. In contrast, we show that PF-04217903 is $>$1000-fold selective for an overlapping panel of 208 kinases. While both PF-02341066 and PF-04217903 are highly selective against a large panel of diverse kinases, PF-04217903 has an exceptionally high level of kinase selectivity. When evaluating the inhibition of c-Met mutant proteins biochemically, PF-02341066 had a higher tolerance for variation. This observation was confirmed biophysically by measuring the alteration of melting temperature. The trend in the magnitude of the T_m shifts upon compound binding to mutant c-Met proteins was found to be similar to inhibition potency (K_i) results. Inhibition of a subset of c-Met mutants in a cellular context was consistent with the biochemical observations.

Crystal structures of wild-type c-Met bound to inhibitors can help in understanding the inhibition data of these inhibitors to c-Met mutants. Crystal structures of PF-02341066 (PDB entry 2wgj) and triazolopyrazine compounds (PDB entries 3CCN and 3CD8) bound to c-Met kinase domain show that both classes of inhibitors bind to a similar conformation of c-Met (Figure 4). Several of the mutation sites are in or near the inhibitor binding site (Figure 4). In particular, the side chain of tyrosine 1230 makes direct contact with the dichlorofluorophenyl ring of PF-02341066 and the triazolopyrazine ring of the PF-04217903 series inhibitors. It is therefore not surprising that mutations of tyrosine 1230 result in a loss or reduction of inhibitory activity of these compounds as in these mutants the loss or decrease in this direct interaction is predicted to decrease inhibitor binding affinity.

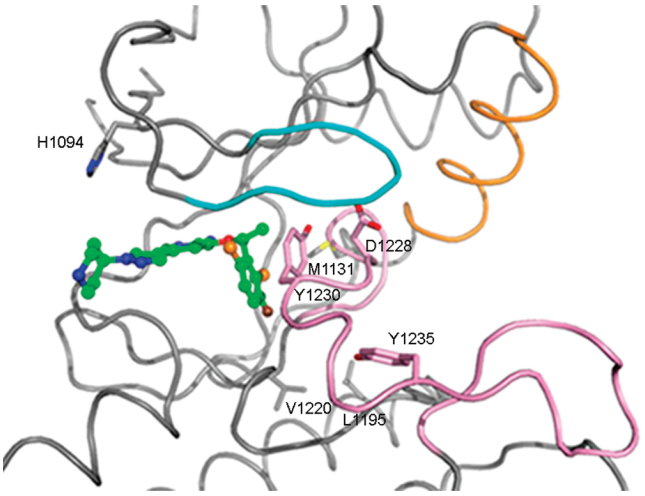

FIGURE 4: Crystal structure of PF-02341066 bound to the kinase domain of c-Met (PDB entry 2wgj). Side chain atoms are shown for selected oncogenic mutation sites. The protein fold coloring is as follows: overall (gray), activation loop (pink), α helix C (orange), and glycine-rich loop (cyan). The atom coloring is as follows: nitrogen (blue), oxygen (red), sulfur (yellow), chlorine (gold), fluorine (brown), and PF-02341066 carbon atoms (green).

This study uses a combination of enzymatic, biophysical, structural, and cellular methods in the characterization of specific, optimized small molecule inhibitors to unveil complex biological interactions critical to understanding receptor tyrosine kinase biology and design of therapeutic agents. The study highlights the need to understand the molecular underpinnings of inhibitor interactions to identify optimal therapeutic agents. For kinases that are susceptible to activating mutations in the disease state, either naturally occurring or through acquired resistance to drug therapy, care must be taken to balance overall kinase selectivity with potency for various mutations.

ACKNOWLEDGMENT

We gratefully acknowledge Stephan Grant for critically reading the manuscript and offering valued opinions.

SUPPORTING INFORMATION AVAILABLE

Tables of kinase selectivity data for PF-04217903. This material is available free of charge via the Internet at http://pubs.acs.org.

REFERENCES

1. Bottaro, D. P., Rubin, J. S., Faletto, D. L., Chan, A. M., Kmiecik, T. E., Vande Woude, G. F., and Aaronson, S. A. (1991) Identification of the hepatocyte growth factor receptor as the c-met proto-oncogene product. *Science 251*, 802–804.
2. Naldini, L., Vigna, E., Narsimhan, R. P., Gaudino, G., Zarnegar, R., Michalopoulos, G. K., and Comoglio, P. M. (1991) Hepatocyte growth factor (HGF) stimulates the tyrosine kinase activity of the receptor encoded by the proto-oncogene c-MET. *Oncogene 6*, 501–504.
3. Liu, X., Yao, W., Newton, R. C., and Scherle, P. A. (2008) Targeting the c-MET signaling pathway for cancer therapy. *Expert Opin. Invest. Drugs 17*, 997–1011.
4. Maulik, G., Shrikhande, A., Kijima, T., Ma, P. C., Morrison, P. T., and Salgia, R. (2002) Role of the hepatocyte growth factor receptor,

c-Met, in oncogenesis and potential for therapeutic inhibition. *Cytokine Growth Factor Rev. 13*, 41–59.
5. Naldini, L., Vigna, E., Ferracini, R., Longati, P., Gandino, L., Prat, M., and Comoglio, P. M. (1991) The tyrosine kinase encoded by the MET proto-oncogene is activated by autophosphorylation. *Mol. Cell. Biol. 11*, 1793–1803.
6. Longati, P., Bardelli, A., Ponzetto, C., Naldini, L., and Comoglio, P. M. (1994) Tyrosines 1234−1235 are critical for activation of the tyrosine kinase encoded by the MET proto-oncogene (HGF receptor). *Oncogene 9*, 49–57.
7. Cristiani, C., Rusconi, L., Perego, R., Schiering, N., Kalisz, H. M., Knapp, S., and Isacchi, A. (2005) Regulation of the wild-type and Y1235D mutant Met kinase activation. *Biochemistry 44*, 14110–14119.
8. Chiara, F., Michieli, P., Pugliese, L., and Comoglio, P. M. (2003) Mutations in the met oncogene unveil a "dual switch" mechanism controlling tyrosine kinase activity. *J. Biol. Chem. 278*, 29352–29358.
9. Hays, J. L., and Watowich, S. J. (2003) Oligomerization-induced modulation of TPR-MET tyrosine kinase activity. *J. Biol. Chem. 278*, 27456–27463.
10. Sheth, P. R., Hays, J. L., Elferink, L. A., and Watowich, S. J. (2008) Biochemical basis for the functional switch that regulates hepatocyte growth factor receptor tyrosine kinase activation. *Biochemistry 47*, 4028–4038.
11. Knudsen, B. S., and Vande Woude, G. (2008) Showering c-MET-dependent cancers with drugs. *Curr. Opin. Genet. Dev.*, 87–96.
12. Dussault, I., and Bellon, S. F. (2009) From concept to reality: The long road to c-Met and RON receptor tyrosine kinase inhibitors for the treatment of cancer. *Anticancer Agents Med. Chem. 9*, 221–229.
13. Schmidt, L., Duh, F. M., Chen, F., Kishida, T., Glenn, G., Choyke, P., Scherer, S. W., Zhuang, Z., Lubensky, I., Dean, M., Allikmets, R., Chidambaram, A., Bergerheim, U. R., Feltis, J. T., Casadevall, C., Zamarron, A., Bernues, M., Richard, S., Lips, C. J., Walther, M. M., Tsui, L. C., Geil, L., Orcutt, M. L., Stackhouse, T., Lipan, J., Slife, L., Brauch, H., Decker, J., Niehans, G., Hughson, M. D., Moch, H., Storkel, S., Lerman, M. I., Linehan, W. M., and Zbar, B. (1997) Germline and somatic mutations in the tyrosine kinase domain of the MET proto-oncogene in papillary renal carcinomas. *Nat. Genet. 16*, 68–73.
14. Di Renzo, M. F., Olivero, M., Martone, T., Maffe, A., Maggiora, P., Stefani, A. D., Valente, G., Giordano, S., Cortesina, G., and Comoglio, P. M. (2000) Somatic mutations of the MET oncogene are selected during metastatic spread of human HNSC carcinomas. *Oncogene 19*, 1547–1555.
15. Jeffers, M., Schmidt, L., Nakaigawa, N., Webb, C. P., Weirich, G., Kishida, T., Zbar, B., and Vande Woude, G. F. (1997) Activating mutations for the met tyrosine kinase receptor in human cancer. *Proc. Natl. Acad. Sci. U.S.A. 94*, 11445–11450.
16. Jeffers, M. F. (1999) Activating mutations in the Met receptor overcome the requirement for autophosphorylation of tyrosines crucial for wild type signaling. *Oncogene 18*, 5120–5125.
17. Schmidt, L., Junker, K., Nakaigawa, N., Kinjerski, T., Weirich, G., Miller, M., Lubensky, I., Neumann, H. P., Brauch, H., Decker, J., Vocke, C., Brown, J. A., Jenkins, R., Richard, S., Bergerheim, U., Gerrard, B., Dean, M., Linehan, W. M., and Zbar, B. (1999) Novel mutations of the MET proto-oncogene in papillary renal carcinomas. *Oncogene 18*, 2343–2350.
18. Graveel, C., Su, Y., Koeman, J., Wang, L. M., Tessarollo, L., Fiscella, M., Birchmeier, C., Swiatek, P., Bronson, R., and Vande Woude, G. (2004) Activating Met mutations produce unique tumor profiles in mice with selective duplication of the mutant allele. *Proc. Natl. Acad. Sci. U.S.A. 101*, 17198–17203.
19. Peruzzi, B., and Bottaro, D. P. (2006) Targeting the c-Met signaling pathway in cancer. *Clin. Cancer Res. 12*, 3657–3660.
20. Christensen, J. G., Zou, H. Y., Arango, M. E., Li, Q., Lee, J. H., McDonnell, S. R., Yamazaki, S., Alton, G. R., Mroczkowski, B., and Los, G. (2007) Cytoreductive antitumor activity of PF-2341066, a novel inhibitor of anaplastic lymphoma kinase and c-Met, in experimental models of anaplastic large-cell lymphoma. *Mol. Cancer Ther. 6*, 3314–3322.
21. Zou, H. Y., Li, Q., Lee, J. H., Arango, M. E., McDonnell, S. R., Yamazaki, S., Koudriakova, T. B., Alton, G., Cui, J. J., Kung, P. P., Nambu, M. D., Los, G., Bender, S. L., Mroczkowski, B., and Christensen, J. G. (2007) An orally available small-molecule inhibitor of c-Met, PF-2341066, exhibits cytoreductive antitumor efficacy through antiproliferative and antiangiogenic mechanisms. *Cancer Res. 67*, 4408–4417.
22. Murray, B. W., Padrique, E. S., Pinko, C., and McTigue, M. A. (2001) Mechanistic effects of autophosphorylation on receptor tyrosine kinase catalysis: Enzymatic characterization of Tie2 and phospho-Tie2. *Biochemistry 40*, 10243–10253.
23. Stein, B., Yang, M. X., Young, D. B., Janknecht, R., Hunter, T., Murray, B. W., and Barbosa, M. S. (1997) p38-2, a novel mitogen-activated protein kinase with distinct properties. *J. Biol. Chem. 272*, 19509–19517.
24. Lukovic, E., Gonzalez-Vera, J. A., and Imperiali, B. (2008) Recognition-domain focused chemosensors: Versatile and efficient reporters of protein kinase activity. *J. Am. Chem. Soc. 130*, 12821–12827.
25. Pantoliano, M. W., Petrella, E. C., Kwasnoski, J. D., Lobanov, V. S., Myslik, J., Graf, E., Carver, T., Asel, E., Springer, B. A., Lane, P., and Salemme, F. R. (2001) High-density miniaturized thermal shift assays as a general strategy for drug discovery. *J. Biomol. Screening 6*, 429–440.
26. Vedadi, M., Niesen, F. H., Allali-Hassani, A., Fedorov, O. Y., Finerty, P. J.Jr., Wasney, G. A., Yeung, R., Arrowsmith, C., Ball, L. J., Berglund, H., Hui, R., Marsden, B. D., Nordlund, P., Sundstrom, M., Weigelt, J., and Edwards, A. M. (2006) Chemical screening methods to identify ligands that promote protein stability, protein crystallization, and structure determination. *Proc. Natl. Acad. Sci. U. S.A. 103*, 15835–15840.
27. Parast, C. V., Mroczkowski, B., Pinko, C., Misialek, S., Khambatta, G., and Appelt, K. (1998) Characterization and kinetic mechanism of catalytic domain of human vascular endothelial growth factor receptor-2 tyrosine kinase (VEGFR2 TK), a key enzyme in angiogenesis. *Biochemistry 37*, 16788–16801.
28. Gotoh, N., Tojo, A., Hino, M., Yazaki, Y., and Shibuya, M. (1992) A highly conserved tyrosine residue at codon 845 within the kinase domain is not required for the transforming activity of human epidermal growth factor receptor. *Biochem. Biophys. Res. Commun. 186*, 768–774.
29. Craciun, G., Tang, Y., and Feinberg, M. (2006) Understanding bistability in complex enzyme-driven reaction networks. *Proc. Natl. Acad. Sci. U.S.A. 103*, 8697–8702.
30. Krishnamurthy, S., Smith, E., Krakauer, D., and Fontana, W. (2007) The stochastic behavior of a molecular switching circuit with feedback. *Biol. Direct 2*, 13.
31. Lisman, J. E. (1985) A mechanism for memory storage insensitive to molecular turnover: A bistable autophosphorylating kinase. *Proc. Natl. Acad. Sci. U.S.A. 82*, 3055–3057.